Published on 29 September 2017. Downloaded by Changchun Institute of Optics, Fine Mechanics and Physics, CAS on 31/05/2018 09:42:26.

Journal of
Materials Chemistry C

PAPER

View Article Online
View Journal | View Issue

Check for updates

Cite this: J. Mater. Chem. C, 2017, 5, 11076

Energy transfer assisted solvent effects on $CsPbBr_3$ quantum dots†

Jingjing Mei,[ab] Fei Wang,*[a] Yunpeng Wang,[a] Cancan Tian,[ab] Hongzhen Liu[ab] and Dongxu Zhao*[a]

Received 26th July 2017,
Accepted 28th September 2017

DOI: 10.1039/c7tc03351f

rsc.li/materials-c

In this work, the solvent effects of chemically synthesized $CsPbBr_3$ quantum dots (QDs) were investigated by dissolving the QDs into solvents of different polarities. The QDs exhibited green fluorescence in non-polar solvents like 1-octadecene, hexane and ether, but exhibited blue fluorescent color in solvents of higher polarities (ethanol or acetone). The photoluminescence (PL), Fourier transform infrared (FTIR), transmission electron microscope (TEM) and time-resolved PL characterization revealed the difference between QDs in the two types of solvents. The hydrogen bonding system of $-NH_2$ and polar solvents was responsible for the different fluorescent colors. Also, energy transfer between the QDs and the hydrogen bonding system was observed and confirmed by using ultrafast femtosecond transient absorption spectroscopy. We expect that the solvent effects of $CsPbBr_3$ QDs have potential applications in fluorescence probes and photoelectrical devices.

Introduction

As a new type of semiconductor material, lead halide perovskites exhibit superb properties such as ultrafast charge generation, high mobility, long charge carrier lifetime *etc.*, and therefore have attracted much attention recently. Organometal halide perovskites have shown outstanding performance in the applications of solar cells.[1,2] In 2015, scientists fabricated a formamidinium lead iodide perovskite ($FAPbI_3$) based solar cell, whose maximum conversion efficiency was greater than 20%.[3] Moreover, studies of organic–inorganic complex perovskites have extended into the field of optoelectronic devices such as field-effect transistors[4] and memristors.[5] However, they also have many obvious deficiencies resulting from unsolved photo-stability and low fluorescence quantum yield (QY), which have limited applications in luminescent devices. Maksym V. Kovalenko *et al.* have designed and synthesized highly luminescent inorganic perovskite quantum dots (QDs) ($CsPbX_3$, X = Cl, Br, I) with a QY of up to 90%.[6,7] Compared with organometal halide perovskites, they exhibit better photo-stability and more easily adjustable fluorescence spectra, which benefit from the size effect and surface effect of QD materials. In addition, the emission wavelength of the inorganic perovskite QDs can not only be tuned by changing the size of the nanoparticles, but also be adjusted by fast inter-nanocrystal anion-exchange processes.[8,9] Because of the advantages mentioned above, the $CsPbX_3$ QDs have shown great potential in various optoelectronic devices such as light-emitting diodes (LEDs),[10] detectors[11] and so on.

In QD materials, surface ligands that are introduced during the synthesis process have played crucial roles in their performances.[12–15] The environmental conditions of the QDs in solution have a major impact on the surface ligands, and therefore they influence the dispersibility, stability and photoelectric properties of the QDs.[16–19] In particular the polarity of the solvent has been widely discussed.[20–23] Ibnauf *et al.* have reported that the photoluminescence (PL) at 590 nm of CdSe QDs was quenched when they were dissolved in a highly polar solvent.[24] In 2016, amphiphilic carbon dots were synthesized and tunable PL from blue to orange by changing the solvent has been observed.[25] Furthermore, the solvent effects of QDs were also applied in the fabrication and improvement of optoelectronic devices.[26,27] Kirmani *et al.* reported that high dipole moment aprotic solvents like acetonitrile improved the performances of solar cells fabricated by colloidal QDs. By exploiting the interactions of solvents and QD films they greatly simplified the active layer deposition.[28] Therefore, research on the solvent influence on QD materials cannot be neglected.

In this work, the solvent effects of $CsPbBr_3$ QDs were investigated by dispersing the QDs into solvents of different polarity, and the variation in the fluorescent color was observed from the PL spectra of the QDs in hexane, 1-octadecene, ether, acetone and ethanol. The Fourier transform infrared (FTIR) spectra of the QDs revealed the differences in the surface

[a] State Key Laboratory of Luminescence and Applications, Changchun Institute of Optics, Fine Mechanics and Physics, Chinese Academy of Sciences, 3888 Dongnanhu Road, Changchun 130021, People's Republic of China. E-mail: wangf@ciomp.ac.cn, zhaodx@ciomp.ac.cn; Tel: +86-431-86708227
[b] University of Chinese Academy of Sciences, Beijing 100049, People's Republic of China

† Electronic supplementary information (ESI) available. See DOI: 10.1039/c7tc03351f

This journal is © The Royal Society of Chemistry 2017

Published on 29 September 2017. Downloaded by Changchun Institute of Optics, Fine Mechanics and Physics, CAS on 31/05/2018 09:42:26.

groups in different solvents. The fluorescence, which originated from the intrinsic luminescence of the QDs and the hydrogen bonding system of $-NH_2$ and the polar solvents, was investigated and confirmed. The energy transfer process between these two luminous centers has been observed and studied by using time-resolved PL curves and ultrafast femtosecond transient absorption spectroscopy. This work might extend the potential applications of $CsPbBr_3$ QDs in device fabrication, molecular recognizers and so on.

Experimental

Preparation of Cs-oleate

$CsPbBr_3$ QDs were prepared by a chemical synthesis method. In order to prevent them from being oxidized, all reactions were performed in a glove box under the protection of N_2. Cs-oleate was synthesized first, which is the precursor of $CsPbBr_3$. 0.8 g $CsCO_3$ (Aladdin, 99%), 30 ml 1-octadecene (Aladdin, ≥95%) and 2.5 ml oleic acid (Sinopharm Chemical Reagents, AR) were put into a three-necked flask, and dried under vacuum at a temperature of 120 °C for 3 h. Then the flask was transferred into a glove box and heated to 150 °C. When the color of the solution changed to dark brown, the reaction was complete. Before being used, it needed to be heated to 120 °C again.

Synthesis of $CsPbBr_3$ QDs

0.138 g $PbBr_2$ (Aladdin, 99%), 10 ml 1-octadecene, 1 ml oleylamine and 1 ml oleic acid were loaded into a 50 ml three-necked flask and heated at 120 °C with stirring under an N_2 atmosphere. When $PbBr_2$ was dissolved completely, the reaction temperature was increased to 180 °C. The Cs-oleate which had been heated to 120 °C was injected into the three-necked flask quickly. 5 s later, the reaction flask was cooled in an ice-water bath.

Reprecipitation of $CsPbBr_3$ QDs

$CsPbBr_3$ QDs of suitable sizes were obtained by centrifugation. The reaction solution which was received above was centrifuged for 10 min with a speed of 9000 rpm, and then the supernatant was collected. To maximally protect the surface ligand density of the QDs from decreasing, ethyl acetate was used for the purification process. The supernatant was added into ethyl acetone (Sinopharm Chemical Reagents, ≥99.5%) with a volume ratio of 1:2, and then the precipitates were collected after 15 min of centrifugation at 9000 rpm. Equal amounts of precipitates were dispersed into 2 ml hexane (Sinopharm Chemical Reagents, ≥95.5%), 1-octadecene, absolute ether (Beijing Chemical Works, 99%), ethanol (Beijing Chemical Works, ≥99.8%) and acetone (Sinopharm Chemical Reagents, ≥99.5%).

Characterization

High resolution transmission electron microscopy (HRTEM) was performed with JEOL JEM-2100F equipment. The PL measurement was carried out with a Hitachi F-7000 fluorescence spectrophotometer, and the absorption spectra were recorded using a Shimadzu UV-3101 PC spectrophotometer. The FTIR spectrum was recorded with a Bruker VERTEX spectrometer. X-ray diffraction (XRD) patterns were collected with a Bruker D8 system. The time-resolved phosphorescence spectra were investigated using an Edinburgh FLS920 fluorescence spectrometer. The light pulses (800 nm, 35 fs, 1 kHz repetition rate) of the ultrafast femtosecond transient absorption spectra were generated by a regenerative amplifier (Spitfire Ace) seeded by a femtosecond oscillator (Mai Tai, spectra physics). The fundamental output of the laser was split into two beams. One was used to generate the pump pulses (360 nm) by an optical parametric amplifier (Tropas, spectra physics), the other (1 μJ per pulse) was focused onto water to generate the probe light. The whole experiment was done at room temperature.

Results and discussion

Fig. 1 shows the corresponding fluorescence and absorption spectra of $CsPbBr_3$ QDs dispersed in different solvents. As can be seen from Fig. 1a, under the illumination of a 365 nm UV lamp, the $CsPbBr_3$ QDs mainly present two types of fluorescent colors: green and blue. The $CsPbBr_3$ QDs dissolved in hexane, 1-octadecene and ether exhibit green fluorescence, showing only one fluorescence peak at approximately 510 nm (as shown in Fig. 1d–f). The full width at half maximum (FWHM) of their emission peaks is as narrow as 15 nm. But when the QDs are dissolved in acetone and ethanol (Fig. 1b and c), they not only show intrinsic luminescence at 510 nm, but also present another peak which can move gradually with an increase in the excitation wavelength. When the QDs dissolved in acetone

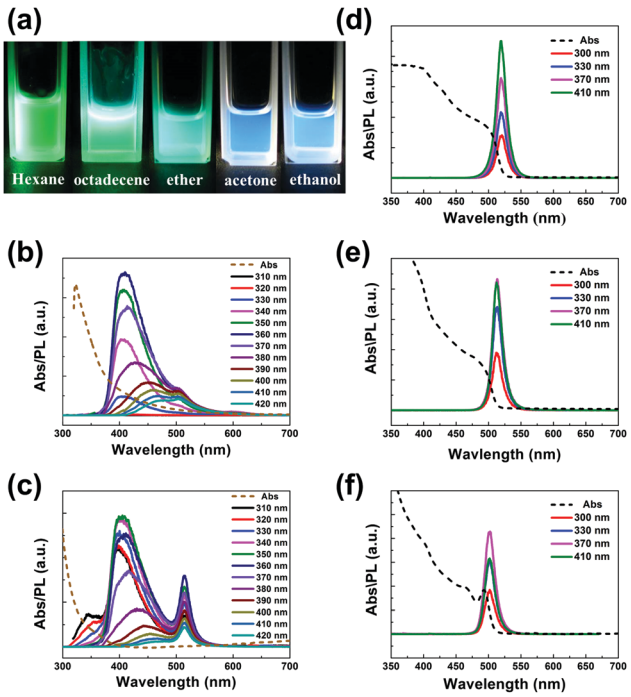

Fig. 1 (a) $CsPbBr_3$ QDs with different solvents under a UV lamp (λ = 365 nm); UV-vis absorption and fluorescence spectra of $CsPbBr_3$ QDs dissolved in acetone (b)/ethanol (c)/hexane (d)/1-octadecene (e)/ether (f).

Published on 29 September 2017. Downloaded by Changchun Institute of Optics, Fine Mechanics and Physics, CAS on 31/05/2018 09:42:26.

and ethanol are excited under illumination ranging from 310 to 420 nm with an interval of 10 nm, the PL peak shifts from 400 nm to 450 nm. Also, the intensity of the peak reduces significantly. The solution presents a blue fluorescent color under the illumination of the UV lamp. In addition, the UV-vis absorption spectra in Fig. 1b and c are changed dramatically compared to Fig. 1d–f, and the absorption edges are blue-shifted from 510 nm to 350–450 nm, which indicates the formation of new luminescent centers when the QDs are dissolved in acetone and ethanol.[29]

This phenomenon has not been reported in inorganic perovskites before, but similar properties have been observed in other nanoparticles like carbon dots.[30,31] The appearance of this phenomenon may be closely related to the different solvents which could affect the surface of the $CsPbBr_3$ QDs. In order to explore the surface groups, the corresponding FTIR spectra of the QD thin films spin-coated onto KBr substrates were measured and shown in Fig. 2. The peaks at 2854 cm^{-1} and 2924 cm^{-1} in Fig. 2a–d can be assigned to ν(C–H) of methylene. The peaks at 3078 cm^{-1} can be attributed to ν(C–H) of olefin. The peaks at 1639 cm^{-1} originate from ν(C=C). So we can be sure that all of these solutions contain olefin, which is the residual 1-octadecene solvent. The bands between 1000 and 675 cm^{-1} can be attributed to δ(C–H). The peaks at 721 cm^{-1} are characteristic peaks of $-(CH2)_n-$ in long chain saturated hydrocarbons. All of the peaks mentioned above are observed in all the spectra. But when the $CsPbBr_3$ QDs are dissolved in acetone and ethanol, peaks at 3700 cm^{-1} in Fig. 2d and e can be observed, which have not been found in hexane and ether solution. These peaks indicate the presence of ν(N–H) in $-NH_2$. So in ethanol and acetone, the $CsPbBr_3$ QDs are wrapped in a small amount of amino surfactant groups. The amino groups come from oleylamine, which is the surfactant of the main reaction. The X-ray photoelectron spectroscopy (XPS) spectra of the QDs in Fig. S1c, f and i (ESI†) show N 1s peaks at ~400 eV, which confirms the existence of $-NH_2$ groups on the surface of the QDs. Meanwhile, the intensities of the N 1s peaks in Fig. S1f and i (ESI†) present a two fold enhancement compared to Fig. S1c (ESI†), which indicates that the number of surface groups increased when the QDs were dissolved in ethanol and acetone. These organic groups could interact with the solvent easily,[32] so the fluorescence spectra of the QDs in acetone and ethanol (Fig. 1b and c) show different luminescence phenomena.

In addition, to investigate the microstructure of the $CsPbBr_3$ QDs in different solvents, TEM images of the QDs in different solvents were recorded and shown in Fig. 3. From the picture, it can be seen clearly that the QDs in different solvents show dissimilar morphologies. As shown in Fig. 3a and b, the QDs in ethanol aggregate together and the aggregations are coated with organics. In contrast, the QDs dissolved in hexane (Fig. 3c) with a diameter of 10 nm can be observed clearly, and are arranged in an orderly manner without any sign of aggregation. This is consistent with the observations from the FTIR spectra and the dynamic light scattering (DLS) results (Fig. S2, ESI†) of the QDs dissolved in different solvents. Also, the high-resolution TEM image of the $CsPbBr_3$ QDs in hexane (Fig. 3d) reveals the uniform shape of the QDs with well-resolved lattice fringes, which demonstrates the highly crystalline nature of the QDs. Previous research has indicated that $CsPbBr_3$ QDs in polar solvents can't maintain stability, and can be resolved easily.[33] The degradation process was observed and recorded by fluorescence spectra (Fig. S3, ESI†). From the spectra we learnt that the fluorescence intensity of the solution becomes weak markedly and the peak becomes wide after the $CsPbBr_3$ QDs were dispersed in ethanol or acetone for 10 days, which indicates that the QDs have begun to degrade. However, the degradation of the $CsPbBr_3$ QDs in ethanol or acetone needs a certain period of time. In order to ensure the structural integrity of $CsPbBr_3$ QDs, all the measurements were completed in three days after the preparation of the samples. The X-ray diffraction (XRD) patterns of $CsPbBr_3$ QDs dispersed in ethanol and acetone for 3 days were collected and are shown in Fig. 4. The XRD spectrum of the QDs before polar solvent

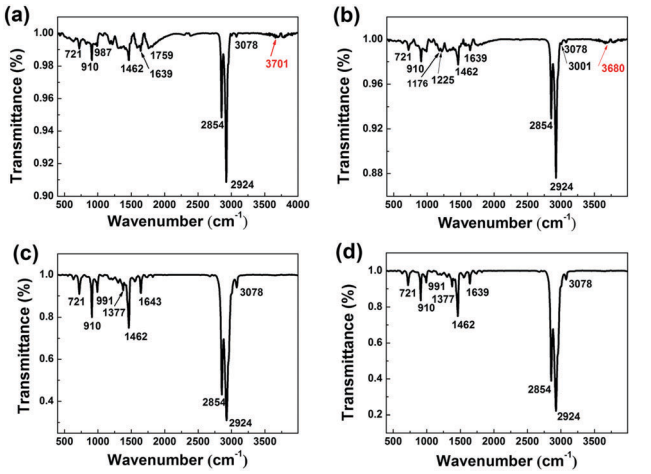

Fig. 2 The ATR-FTIR spectrum of $CsPbBr_3$ QDs dissolved in different solvents. (a: acetone; b: ethanol; c: ether; d: hexane).

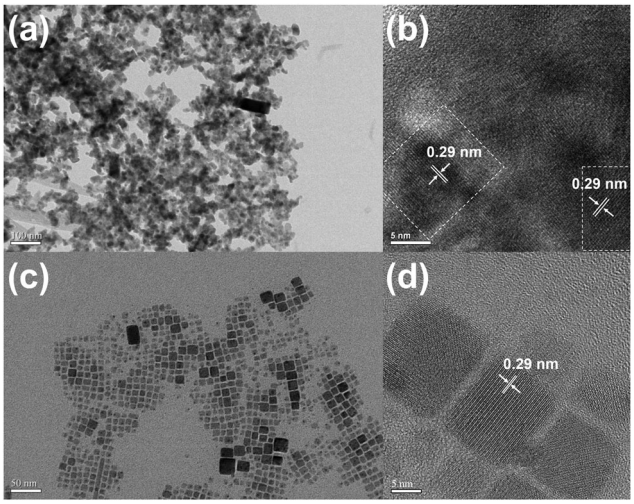

Fig. 3 Typical TEM images of $CsPbBr_3$ QDs dissolved in ethanol (a and b) and hexane (c and d).

 This journal is © The Royal Society of Chemistry 2017

Published on 29 September 2017. Downloaded by Changchun Institute of Optics, Fine Mechanics and Physics, CAS on 31/05/2018 09:42:26.

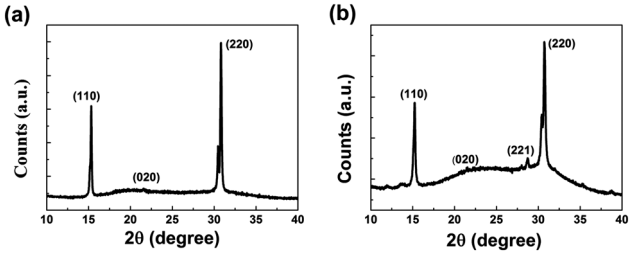

Fig. 4 XRD patterns of $CsPbBr_3$ QDs dispersed in solvents of ethanol (a) and acetone (b) for 3 days.

treatments is also shown in Fig. S4 (ESI†). The diffraction peaks in Fig. 4 and Fig. S4 (ESI†) prove that the QDs are $CsPbBr_3$ (ICSD 97851).[34–36] Moreover, the XPS spectra show peaks of Br 3d and Cs 3d (Fig. S1, ESI†), which are consistent with the literature on $CsPbBr_3$ QDs.[36–39] The characterizations mentioned above indicate that the $CsPbBr_3$ QDs dissolved in ethanol and acetone did not degrade during our experimental period.

From strong to weak, the order of polarity for the five solvents is ethanol, acetone, ether, 1-octadecene, and hexane. Because of the different polarities, the charge distribution of the solvent molecules was also different. Both acetone and ethanol are strongly polar molecules, and their negative charges are mainly accumulated on oxygen-containing groups like carbonyl (–C═O) and hydroxyl (–OH).[40] Therefore, it is easy for them to form hydrogen bonding with amino groups ($-NH_2$) in solution.[41] Also, because the oxygen atoms have a much stronger electronegativity than the nitrogen atom,[42] they can attract more charges of $-NH_2$ and reduce the charge density of $-NH_2$. So the $-NH_2$ can be easily absorbed on the surface of the $CsPbBr_3$ QDs. This is similar to the adsorption of thiol on the surface of Au nanoparticles.[43] The oxygen-containing groups and surface groups interact with each other, which leads to the formation of the hydrogen bonding system, and then results in the fluorescence from 350 to 450 nm.[29,44] Hexane is a nonpolar solvent. For 1-octadecene and ether, their polarity is too weak to connect with $-NH_2$. As a result, the QDs dissolved in them cannot adsorb $-NH_2$ groups on the surface. So from the IR spectra in Fig. 2 we did not observe the ν(N–H) of oleylamine on the surface of the QDs in hexane, 1-octadecene and ether.

The PL spectra of the QD thin films were investigated to eliminate the influence of the different solvents on the $CsPbBr_3$ QDs. The QD solutions in different solvents were dropped onto glass substrates and then dried in a vacuum oven at 60 °C. The corresponding PL spectra are shown in Fig. 5a and b. The peaks at approximately 510 nm are significantly enhanced. Yet, the peaks at 350–450 nm are much weaker and even disappeared. It is further confirmed that the PL peaks ranging from 350 nm to 450 nm are the result of the interaction between surface groups and solvents. Moreover, the significant enhancement of the PL peak at 510 nm and the simultaneous reduction of the PL intensity at 350–450 nm indicate that there might be energy transfer between them.[45] Fig. 5c shows the fluorescence spectra of $CsPbBr_3$ QDs dissolved in hexane (blue line) and acetone (black line) (concentrations are the same). Fig. 5c (red line)

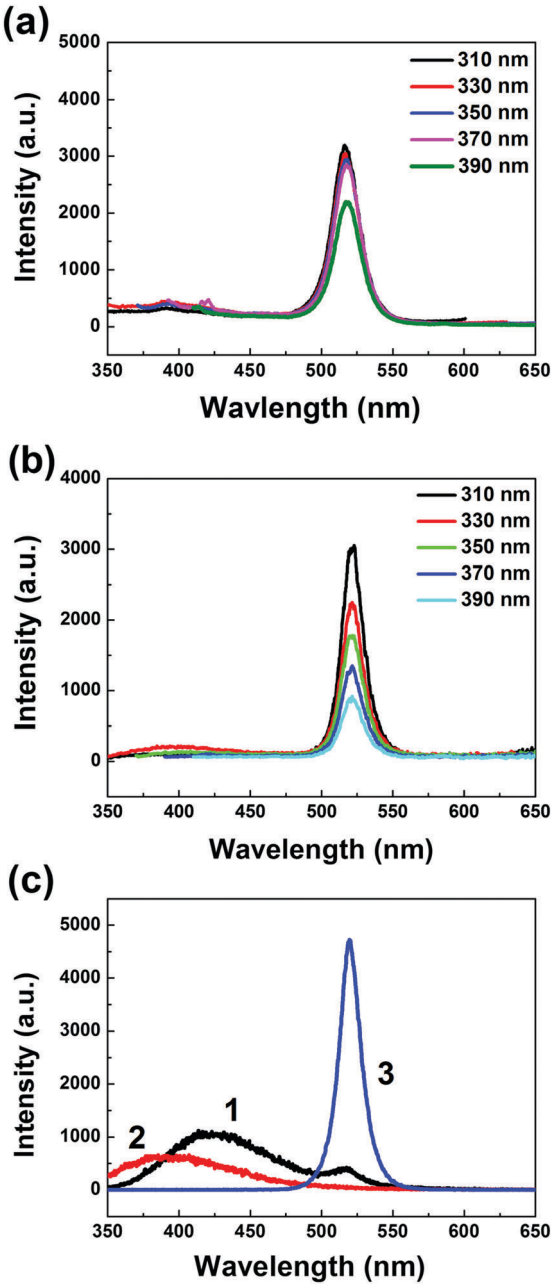

Fig. 5 Fluorescence spectra of $CsPbBr_3$ QDs dissolved in ethanol (a)/acetone (b) and then spin-coated on glass. (c) Fluorescence spectra of $CsPbBr_3$ QDs dissolved in acetone (1) and hexane (3); oleylamine dissolved in acetone (2).

shows the spectrum of oleylamine dissolved in acetone. Compared to the QDs dissolved in hexane, the intrinsic fluorescence peak at approximately 510 nm is almost quenched when the QDs are dissolved in acetone. In contrast, the fluorescence peak originating from the surface groups is enhanced compared to pure oleylamine in acetone, which implies the close relationship of these two luminous centers.[45,46]

To reveal the relationship between the two luminous centers, the time-resolved photoluminescence spectra of the QDs in different solvents were recorded and shown in Fig. 6. After double

Published on 29 September 2017. Downloaded by Changchun Institute of Optics, Fine Mechanics and Physics, CAS on 31/05/2018 09:42:26.

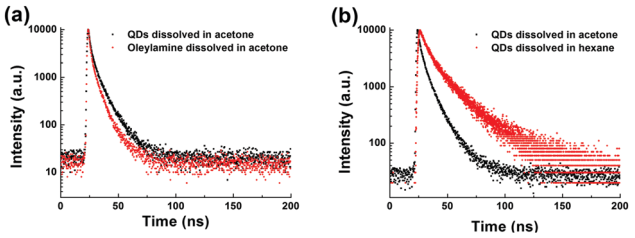

Fig. 6 (a) Time-resolved PL decay for $CsPbBr_3$ QDs dissolved in acetone and oleylamine dissolved acetone (emission peak: 410–440 nm). (b) Time-resolved PL decay for $CsPbBr_3$ QDs dissolved in acetone and hexane (emission peak: 510 nm).

exponent fitting, the corresponding lifetimes are listed in Table 1. The lifetime of the QDs' intrinsic emission at 510 nm is significantly decreased in acetone. However, the PL lifetime of the peaks at 350–450 nm in acetone is increased with the participation of the $CsPbBr_3$ QDs. Due to the absorption of $-NH_2$ groups on the surface, the $CsPbBr_3$ QDs are sufficiently close to the luminescence center, which resulted from the interaction between the solvent and $-NH_2$, and activated the migration of the excitons. Then energy transfer occurs.[47] The sketch in Fig. 7 illustrates the process of energy transfer. As shown in the picture, the hydrogen bonding system of $-NH_2$ and the polar solvents serves as the energy acceptor in the solution, therefore, the PL lifetime and intensity at 350–450 nm are all increased and enhanced after dissolving the $CsPbBr_3$ QDs into acetone. Meanwhile, the QDs play the role of energy donor, which results in the shorter lifetime and the weaker PL intensity of the QDs.

To further confirm the presence of energy transfer, the ultrafast femtosecond transient absorption spectra were recorded to investigate the electron transition dynamics of $CsPbBr_3$ QDs in different solvents (Fig. 8). To achieve a better understanding, the

Table 1 Fitted decay times and normalized amplitudes of the PL emissions of solutions at different wavelengths under 365 nm excitation

Ex: 365 nm	Ex: 365 nm	Em: 510 nm
QDs (hexane)		21.6 ns
QDs (acetone)	8.4 ns	9.2 ns
Oleylamine (acetone)	6.2 ns	

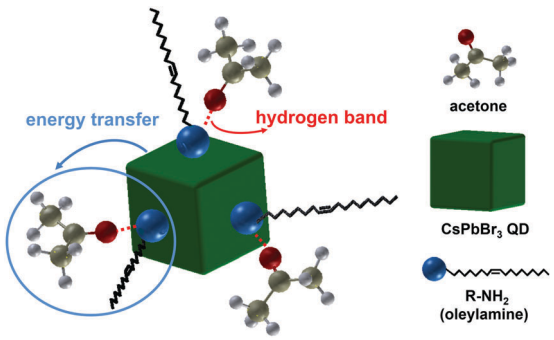

Fig. 7 Schematic representation of the energy transfer process of $CsPbBr_3$ QDs dissolved in acetone.

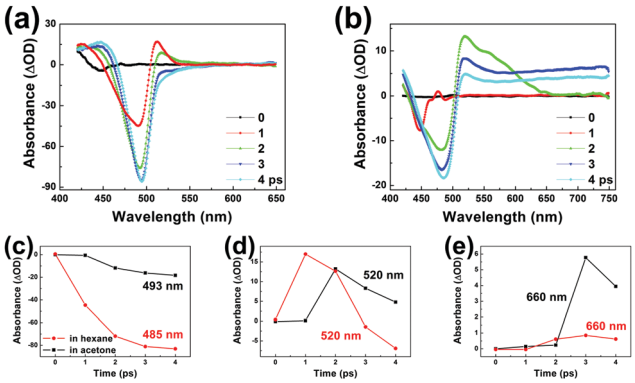

Fig. 8 Ultrafast femtosecond transient absorption spectra of $CsPbBr_3$ QDs dissolved in hexane (a) and acetone (b). (c)–(e) show the time-dependent transient absorption spectra of $CsPbBr_3$ QDs at different wavelengths (red line: in hexane; black line: in acetone).

transient absorption spectra measured from $CsPbBr_3$–hexane solution (Fig. 8a) and $CsPbBr_3$–acetone solution (Fig. 8b) were separated into several components by Singular Value Decomposition (SVD).[48–50] SVD is a useful analysis method for complex spectra with overlapping features. A set of time-resolved spectra measured at m_λ wavelengths and n_t times have been recorded. Let the m by n data matrix A be a collection of spectra

$$A_{i,j} = A(\lambda_i, t_j) \tag{1}$$

For the matrix A of real elements the SVD is defined by the product of three matrices, which is called the SVD of A

$$A = USV^T \tag{2}$$

where the columns of U and V are called the left and right singular vectors of A, respectively. U contains the basis spectra of the data matrix A, which are collected and shown in Fig. 9. The proportions of each spectrum in Fig. 9 after the SVD analysis process are also shown in Fig. S5 (ESI†). There are three major absorption spectra of the $CsPbBr_3$–hexane solution shown in a1–a3 of Fig. 9. In b1–b4 of Fig. 9, it is found that the first three components are almost the same as a1–a3. It is easy to understand that under the same pump pulse, the $CsPbBr_3$ QDs in the two kinds of solution show the same electron transition processes. Fig. 10 shows the energy level diagram deduced from the transient absorption spectra of the $CsPbBr_3$ QDs. The transient absorption bleaching signal located at around 400 nm and 500 nm in a1–a3 and b1–b3 of Fig. 9 can

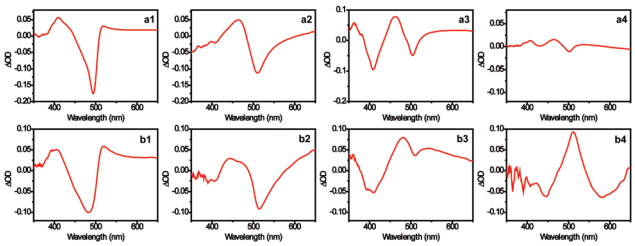

Fig. 9 The ultrafast femtosecond transient absorption spectroscopy of the QDs dissolved in hexane (a1–a4) and acetone (b1–b4).

 This journal is © The Royal Society of Chemistry 2017

Published on 29 September 2017. Downloaded by Changchun Institute of Optics, Fine Mechanics and Physics, CAS on 31/05/2018 09:42:26.

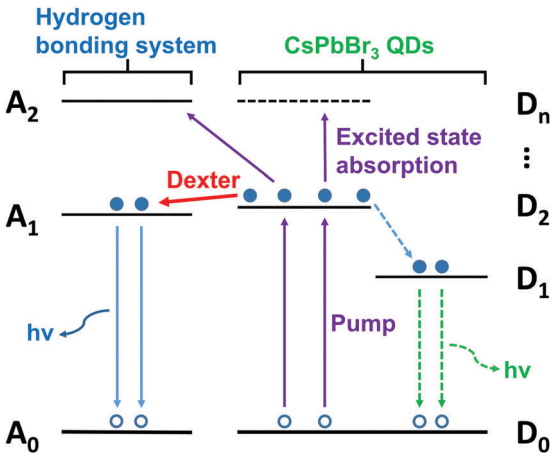

Fig. 10 Energy level diagram depicting the process of energy transfer (dashed line: $CsPbBr_3$ in hexane; solid line: $CsPbBr_3$ in acetone).

be attributed to the state filling of the D_1 and D_2 electron levels in the $CsPbBr_3$ QDs. The dashed lines in Fig. 10 show the electron relaxation process in the $CsPbBr_3$ QDs, which emits photons with a wavelength of 510 nm. Nevertheless, the fourth components of the two samples (a4 and b4 in Fig. 9) are very different, there appears a very strong absorption signal at approximately 500 nm. The existence of the fourth absorption spectra of the QDs dissolved in acetone suggests that an extra electronic transition process has taken place in $CsPbBr_3$–acetone solution, which could be attributed to the absorption of the energy transfer between the QDs and the hydrogen bonding system of $-NH_2$ and acetone. The bleaching signal at about 450 nm in b4 originates from the state filling of the A_1 electron level in the hydrogen bounding system, and the bleaching signal at 575 nm in b4 can be ascribed to the state filling of the A_2 level by the electrons from the D_2 level. The electron levels of A_1 and D_2 have a spatial overlap of the wave functions, and when the electronic excited state within the acceptor (hydrogen bounding system) lies energetically below the excited state of the donor ($CsPbBr_3$ QDs), Dexter energy transfer occurs.[51–53] Fig. 8c–e show the time-dependent transient absorption spectra at different wavelengths. The bleaching signals in Fig. 8c and the absorption signals in Fig. 8d correspond to the state filling and excited state absorption processes in $CsPbBr_3$ QDs respectively, which show similar spectra. This result also indicates that although dissolved in different solvents, the intrinsic electron transition processes in $CsPbBr_3$ QDs have not been affected. However, after 2 ps as shown in Fig. 8e, signals appear in the spectra of $CsPbBr_3$–acetone solution at a wavelength longer than 600 nm, which suggests variation of the valence state. Under the pump pulse of 360 nm used in this work, the solvent itself (hexane or acetone) has no transient absorption signal, and they do not participate in the electron transition processes of the QD solutions. Therefore, the valence state variation may be caused by the Dexter energy transfer from the QDs to the hydrogen bonding system. The results have confirmed that energy transfer occurred from $CsPbBr_3$ QDs to the surface groups, which results in solvent effects of variable fluorescent colors of $CsPbBr_3$ QDs in different solvents.

Conclusion

The solvent effects of chemically synthesized $CsPbBr_3$ QDs were investigated by dissolving the QDs into solvents of different polarities. When dissolved in non-polar and low-polar solvents (1-octadecene, hexane and ether), the QDs exhibited intrinsic fluorescence centered at approximately 510 nm. Yet, when the QDs were dispersed in solvent with high polarities (ethanol or acetone), new peaks ranging from 350 to 450 nm emerged in the PL spectra of the QDs. The fluorescent color of the QDs could be adjusted by changing the solvent. The FTIR spectra were recorded to characterize the surface groups of the QDs, and the hydrogen bonding system of $-NH_2$ and polar solvents was responsible for the fluorescence at 350–450 nm. The variation of the PL intensity and lifetimes under the different states of the QDs suggested the existence of energy transfer between the two luminous centers, which was further confirmed by ultrafast femtosecond transient absorption spectrometry. These novel properties of $CsPbBr_3$ QDs provide a viable source for fluorescence probes and photoelectrical devices.

Conflicts of interest

The authors declare no competing financial interest.

Acknowledgements

This work was supported by the National Natural Science Foundation of China under Grant No. 11504367, and the Youth Scientific Research Foundation of Jilin province under Grant No. 20160520121JH.

References

1 J. Burschka, N. Pellet, S. J. Moon, R. Humphry-Baker, P. Gao, M. K. Nazeeruddin and M. Grätzel, *Nature*, 2013, **499**, 316–320.
2 M. M. Lee, J. Teuscher, T. Miyasaka, T. N. Murakami and H. J. Snaith, *Science*, 2005, **338**, 643–647.
3 W. S. Yang, J. H. Noh, N. J. Jeon, Y. C. Kim, S. Ryu, J. Seo and S. Il. Seok, *Science*, 2015, **348**, 1234–1237.
4 X. Y. Chin, D. Cortecchia, J. Yin, A. Bruno and C. Soci, *Nat. Commun.*, 2015, **6**, 7383.
5 Z. Xiao and J. Huang, *Adv. Electron. Mater.*, 2016, **2**, 1600100.
6 S. Yakunin, L. Protesescu, F. Krieg, M. I. Bodnarchuk, G. Nedelcu, M. Humer, G. D. Luca, M. Fiebig, W. Heiss and M. V. Kovalenko, *Nat. Commun.*, 2015, **6**, 8056.
7 L. Protesescu, S. Yakunin, M. I. Bodnarchuk, F. Krieg, R. Caputo, C. H. Hendon, R. X. Yang, A. Walsh and M. V. Kovalenko, *Nano Lett.*, 2015, **15**, 3692–3696.
8 G. Nedelcu, L. Protesescu, S. Yakunin, M. I. Bodnarchuk, M. J. Grotevent and M. V. Kovalenko, *Nano Lett.*, 2015, **15**, 5635–5640.

Published on 29 September 2017. Downloaded by Changchun Institute of Optics, Fine Mechanics and Physics, CAS on 31/05/2018 09:42:26.

9 B. A. Koscher, N. D. Bronstein, J. H. Olshansky, Y. Bekenstein and A. P. Alivisatos, *J. Am. Chem. Soc.*, 2016, **138**, 12065–12068.
10 J. Pan, L. N. Quan, Y. Zhao, W. Peng, B. Murali, S. P. Sarmah, M. Yuan, L. Sinatra, N. M. Alyami, J. Liu, E. Yassitepe, Z. Yang, O. Voznyy, R. Comin, M. N. Hedhili, O. F. Mohammed, Z. H. Lu, D. H. Kim, E. H. Sarent and O. M. Bakr, *Adv. Mater.*, 2016, **28**, 8718–8725.
11 J. Lu, X. Sheng, G. Tong, Z. Yu, X. Sun, L. Yu, X. Xu, J. Wang, J. Xu, Y. Shi and K. Chen, *Adv. Mater.*, 2017, **29**, 1700400.
12 R. E. Galian and M. D. L. Guardia, *Trends Anal. Chem.*, 2009, **28**, 279–291.
13 B. P. Aryal and D. E. Benson, *J. Am. Chem. Soc.*, 2006, **128**, 15986–15987.
14 Y. Li, C. Pu and X. Peng, *Nano Res.*, 2017, **10**, 941–958.
15 S. A. Fischer, A. M. Crotty, S. V. Kilina, S. A. Ivanov and S. Tretiak, *Nanoscale*, 2012, **4**, 904–914.
16 X. Gao, L. Yang, J. A. Petros, F. F. Marshall, J. W. Simons and S. Nie, *Curr. Opin. Biotechnol.*, 2005, **16**, 63–72.
17 R. Sundheep and R. Prasanth, *J. Mater. Sci.: Mater. Electron.*, 2017, **28**, 3168–3174.
18 C. Bullen and P. Mulvaney, *Langmuir*, 2006, **22**, 3007–3013.
19 V. Biju, R. Kanemoto, Y. Matsumoto, S. Ishii, S. Nakanishi, T. Itoh, Y. Baba and M. Ishikawa, *J. Phys. Chem. C*, 2007, **111**, 7924–7932.
20 Y. S. Liu, Y. Sun, P. T. Vernier, C. H. Liang, S. Y. C. Chong and M. A. Gundersen, *J. Phys. Chem. C*, 2007, **111**, 2872–2878.
21 S. F. Wuister, C. D. M. Donega and A. Meijerink, *J. Am. Chem. Soc.*, 2004, **126**, 10397–10402.
22 J. L. Ellis, D. D. Hickstein, K. J. Schnitzenbaumer, M. B. Wilker, B. B. Palm, J. L. Jimenez, G. Dukovic, H. C. Kapteyn, M. M. Murnane and W. Xiong, *J. Am. Chem. Soc.*, 2015, **137**, 3759–3762.
23 M. F. Torresan, A. M. Baruzzi and R. A. Iglesisa, *Sol. Energy Mater.*, 2017, **164**, 107–113.
24 K. H. Ibnaouf, S. Prasad, M. S. Al Salhi, A. Hamdan, M. B. Zaman and L. El Mir, *J. Lumin.*, 2014, **149**, 369–373.
25 M. Zheng, Y. Li, Y. Zhang and Z. Xie, *RSC Adv.*, 2016, **6**, 83501–83504.
26 C. Jiang, Z. Zhong, B. Liu, Z. He, J. Zou, L. Wang, J. Wang, J. Peng and Y. Cao, *ACS Appl. Mater. Interfaces*, 2016, **8**, 26162–26168.
27 G. Li, H. Wang, T. Zhang, L. Mi, Y. Zhang, Z. Zhang, W. Zhang and Y. Jiang, *Adv. Funct. Mater.*, 2016, **26**, 8478–8486.
28 A. R. Kirmani, G. H. Carey, M. Abdelsamie, B. Yan, D. Cha, L. R. Rollny, X. Cui, E. H. Sargent and A. Amassian, *Adv. Mater.*, 2014, **26**, 4717–4723.
29 Q. Mei, K. Zhang, G. Guan, B. Liu, S. Wang and Z. Zhang, *Chem. Commun.*, 2010, **46**, 7319–7321.
30 S. N. Baker and G. A. Baker, *Angew. Chem., Int. Ed.*, 2010, **49**, 6726–6744.
31 S. Zhu, J. Zhang, C. Qiao, S. Tang, Y. Li, W. Yuan, B. Li, L. Tian, F. Liu, R. Hu, H. Gao, H. Wei, H. Zhang, H. Sun and B. Yang, *Chem. Commun.*, 2011, **47**, 6858–6860.
32 F. Huang, H. Wu, D. Wang, W. Yang and Y. Cao, *Chem. Mater.*, 2004, **16**, 708–716.
33 Y. Kim, E. Yassitepe, O. Voznyy, R. Comin, G. Walters, X. Gong, P. Kanjanaboos, A. F. Nogueira and E. H. Sargent, *ACS Appl. Mater. Interfaces*, 2015, **7**, 25007–25013.
34 Z. Zhu, Q. Yang, L. Gao, L. Zhang, A. Shi, C. Sun, Q. Wang and H. Zhang, *J. Phys. Chem. Lett.*, 2017, **8**, 1610–1614.
35 E. Yao, Z. Yang, L. Meng, P. Sun, S. Dong, Y. Yang and Y. Yang, *Adv. Mater.*, 2017, **29**, 1606859.
36 X. Li, Y. Wu, S. Zhang, B. Cai, Y. Gu, J. Song and H. Zeng, *Adv. Funct. Mater.*, 2016, **26**, 2435–2445.
37 J. Pan, L. N. Quan, Y. Zhao, W. Peng, B. Murali, S. P. Sarmah, M. Yuan, L. Sinatra, N. M. Alyami, J. Liu, E. Yassitepe, Z. Yang, O. Voznyy, R. Comin, M. N. Hedhili, O. F. Mohammed, Z. H. Lu, D. H. Kim, E. H. Sargent and O. M. Bakr, *Adv. Mater.*, 2016, **28**, 8718–8725.
38 F. Palazon, Q. A. Akkerman, M. Prato and L. Manna, *ACS Nano*, 2015, **10**, 1224–1230.
39 S. Seth and A. Samanta, *Sci. Rep.*, 2016, **6**, 37693.
40 J. A. Pople and M. Gordon, *J. Am. Chem. Soc.*, 1967, **89**, 4253–4261.
41 S. F. Sneddon, D. J. Tobias and C. L. Brooks, *J. Mol. Biol.*, 1989, **209**, 817–820.
42 W. Gordy and W. J. O. Thomas, *J. Chem. Phys.*, 1956, **24**, 439–444.
43 Y. Jiang, Y. Huang, H. Cheng, Q. Liu, Z. Xie, T. Yao, Z. Jiang, Y. Huang, Q. Bian, G. Pan, Z. Sun and S. Wei, *J. Phys. Chem. C*, 2014, **118**, 714–719.
44 Y. Lin, J. Gao, H. Liu and Y. Li, *Macromolecules*, 2009, **42**, 3237–3246.
45 N. S. Sariciftci, L. Smilowitz, A. J. Heeger and F. Wudl, *Science*, 1992, **258**, 1474–1476.
46 K. V. Vokhmintcev, P. S. Samokhvalov and I. Nabiev, *Nano Today*, 2016, **11**, 189–211.
47 J. L. Brédas, D. Beljonne, V. Coropceanu and J. Cornil, *Jpn. Chem. Rev.*, 2004, **104**, 4971–5003.
48 R. I. Shrager, *SIAM J. Alg. Discrete Methods*, 1984, **5**, 351–358.
49 R. I. Shrager and R. I. Hendler, *Anal. Chem.*, 1982, **54**, 1147–1152.
50 E. R. Henry and J. Hofrichter, *Methods Enzymol.*, 1992, **210**, 129–192.
51 D. L. Dexter, *J. Chem. Phys.*, 1953, **21**, 836–850.
52 A. Monguzzi, R. Tubino and F. Meinardi, *Phys. Rev. B: Condens. Matter Mater. Phys.*, 2008, **77**, 155122.
53 F. Soler and J. K. McCusker, *J. Am. Chem. Soc.*, 2008, **130**, 4708–4724.

 This journal is © The Royal Society of Chemistry 2017